

Destruction of Malodorous Compounds Using Heterogeneous Photocatalysis

MARIA C. CANELA,
ROSANA M. ALBERICI,
RAQUEL C. R. SOFIA,
MARCOS N. EBERLIN, AND
WILSON F. JARDIM*

*Instituto de Química, Universidade Estadual de Campinas,
CP 6154, CEP 13083-970, Campinas, SP, Brazil*

Photocatalytic oxidation of the sulfur-containing compounds, trimethylene sulfide (C_3H_6S), propylene sulfide (C_3H_6S), thiophene (C_4H_4S), and methyl disulfide ($C_2H_6S_2$), was carried out using an annular plug flow reactor with TiO_2 in a supported form. Formation of products and byproducts was monitored in real time using a mass spectrometry online system. Mineralization of the sulfur-containing compounds was confirmed by mass balance of CO_2 and SO_4^{2-} . Dilute contaminated atmospheres of trimethylene sulfide and propylene sulfide were completely mineralized. For thiophene and methyl disulfide, however, partial oxidation was observed, generating sulfur dioxide (SO_2) and sulfur oxide (SO) as byproducts, which were confirmed by parent ion MS/MS spectra as well as by chemical ionization. Sensory analysis showed that for trimethylene sulfide and propylene sulfide, odor intensity after TiO_2/UV treatment was below the olfactive threshold limit of the panel.

Introduction

The problem with malodorous emissions from sewage and industrial wastewater treatment plants has been largely discussed because it is a nuisance in any neighborhood (1). Sulfur-containing compounds such as mercaptans, organic sulfides, disulfides, and hydrogen sulfide are mainly responsible for obnoxious odors and have an extremely low odor threshold. Malodorous compounds can be associated with odors of different characteristics (fecal, rotten fish, rancid, etc.), according to their functional groups, and are readily detected by the human nose (2, 3). Most techniques of routine analysis are, however, unable to detect odor-causing compounds, hence, their identification is rather difficult even when using the most sophisticated analytical techniques (4). Therefore, sensory analysis is a very useful auxiliary and powerful tool to evaluate hedonistic characteristics of waters and atmospheres.

To control odors, there are several well-established conventional technologies, including adsorption by activated carbon, biofiltration and bioscrubbing, wet chemical scrubbing, thermal oxidation, and prevention. Each of these techniques displays a variety of advantages and disadvantages and different degrees of cost-effectiveness (5). Recently, heterogeneous photocatalysis using TiO_2 as catalyst and near

UV light has attracted interest due to its potential application for the destruction of many pollutants (6, 7). Many of the available studies on TiO_2/UV photocatalysis have been centered on the destruction of volatile organic compounds (VOCs) for atmosphere remediation (8–10). However, the photocatalytic destruction of malodorous compounds has been only slightly explored in the gas phase (11–13).

In this work, we provide preliminary results to help the evaluation of possible application of the TiO_2/UV -vis photocatalytic process for the destruction of malodorous sulfur-containing compounds by monitoring online both target compounds and byproducts using a mass spectrometry system. As the final goal is to lower the compound concentration to a level below the human odor threshold limits, the efficiency of the process was also validated using sensory analysis.

Experimental Section

Titanium dioxide, which was supported in the photocatalytic reactor, as described by Alberici and Jardim (8), was obtained from Degussa (P-25) with an average particle diameter of 30 nm, a crystal structure of primarily anatase, and a surface area of $50 \pm 15 \text{ m}^2 \text{ g}^{-1}$ (BET). The contaminated atmosphere was generated by continuously vaporizing the liquid, in synthetic air. Trimethylene sulfide, propylene sulfide, thiophene, and methyl disulfide (all provided by Aldrich) were used as received in a range of concentration between 20 and 86 ppmv, in synthetic air. Concentration values were chosen considering the background levels of these compounds in the environment and their extremely low odor threshold.

The annular photoreactor consists of a glass cylinder (3.5 cm i.d. \times 86 cm height) and a 30 W black-light lamp (Sankyo Denki Japan-BLB) that serves as the inner surface of the annulus. The internal wall of the glass tube was coated with TiO_2 at a loading density of $9.5 \times 10^{-4} \text{ g/cm}^2$, using a simple soaking/drying coating method. A TiO_2 film thickness of ca. $5.3 \mu\text{m}$ was estimated by the Scanning Electron Micrograph technique (SEM). The UV light intensity at the TiO_2 coating was 4.5 mW cm^{-2} measured by a Cole Parmer radiometer at 365 nm. The photoreactor was fed with synthetic air containing 21% of oxygen and 23% of relative humidity, since water vapor and oxygen are required to maintain long-term catalyst photoactivity (14–17). Experiments were performed in a single pass mode at a flow rate of 250–500 mL min^{-1} , which corresponds to a gas residence time of 1.61–0.81 min at room temperature. No mass transfer limitations were observed when this reactor was used in the destruction of many VOCs, as reported in details by Alberici and Jardim (8). Steady-state conditions were normally achieved after 30 min of UV-irradiation. Conversion rates were monitored using a GC-FID (SHIMADZU GC-14B gas chromatograph) equipped with a DB-624 (30 m \times 0.54 mm \times 3 μm J&W) fused silica megabore column. Experiments under UV irradiation, but in the absence of catalyst, were performed to evaluate conversions owing to photolysis only. A more detailed discussion of the experimental apparatus and procedures is described elsewhere (8).

The destruction of target compounds and the formation of byproducts during the gas-phase photocatalytic oxidation were monitored using a mass spectrometry online monitoring system and selected ion monitoring (SIM). The catalytic photoreactor outlet was connected directly to the gas inlet of an Extrel (Pittsburgh, PA) pentaquadrupole mass spec-

* Corresponding author phone/fax: +55 19 7883135; e-mail: wfjardim@iqm.unicamp.br.

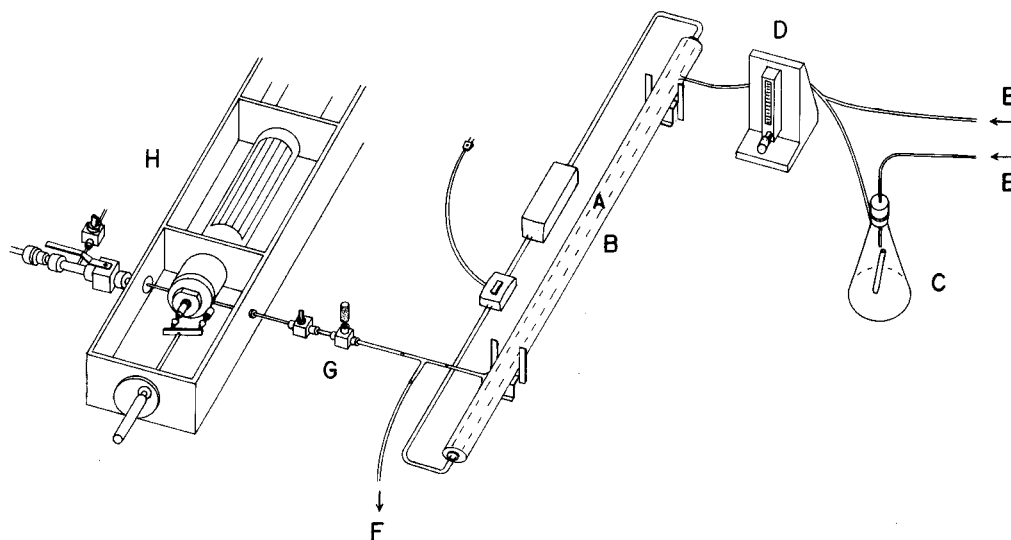


FIGURE 1. Schematic representation of the photocatalytic degradation system and the MS/MS online monitoring: A, black-light lamp; B, photoreactor; C, sulfur-containing compounds reservoir; D, flow meter; E, carrier gas; F, waste; G, needle valve flow control; and H, mass spectrometer.

trometer (18, 19), consisting of three mass analyzers (Q1, Q3, Q5) and two reaction quadrupoles (q2, q4). The gaseous mixture was ionized by either 70 eV electron impact (EI) or chemical ionization (CI). The pentaquadrupole mass spectrometer was also used to help identify products through collision induced dissociation (CID) of mass-selected ions in MS/MS spectrometry. The mass spectrometer is also equipped with a second inlet system, from which known amounts of calibration gases were introduced to quantify the compounds. This procedure was used for target compounds only (Figure 1).

After the photooxidation experiments, the reactor was washed six times with 50 mL of water to remove all adsorbed products. The concentration of sulfate ions was determined by turbidimetry (20). Sulfur dioxide was concentrated by scrubbing through sodium tetrachloromercurate(II) and subsequently determined by colorimetry using *p*-rosaniline (21). Carbon dioxide was monitored in the gas phase using flow injection analysis (FIA) (22). In this method, CO₂ diffuses through a PTFE membrane toward a deionized water stream, forming HCO₃⁻ and H⁺ ions that continuously flow through a conductometric detector. The solution conductance is proportional to the total CO₂ concentration of the gaseous sample.

Sensory analysis was carried out with eight panelists trained to use Flavor Profile Analysis (FPA) (20). Panelists were carefully selected according to their sensitivities to the basic odor and had been trained to sample evaluation and description according to both the Standard Methods for the Examination of Water and Wastewater (20) and Damásio and Costell (23).

Panelists were exposed to the treated atmosphere after the TiO₂/UV and the odor intensity was compared to the initial concentration of the compounds kept in a Tedlar bag. The panelists used a flat scale of 10 cm to register the odor intensity. The flat scale is a horizontal line with two extremities, ranging from weak to strong odor intensity. The panelists score the smell in the outlet reactor after comparing the odor with odor free air and an air sample collected before irradiation. Sensory analyses were carried out only for compounds that were totally mineralized as determined by both mass balance (CO₂ and SO₄²⁻) and MS analysis, to avoid exposing the panelist to possible hazardous compounds formed due to partial destruction of the parent compound.

Results and Discussion

Initial experiments showed that both UV light and TiO₂ were necessary to the oxidation of the sulfur-containing compounds. High levels of destruction of these compounds were measured using both the GC-FID and the mass spectrometry online monitoring system. Figure 2 displays the 70 eV mass spectra obtained before and after UV-irradiation, showing the disappearance of the target compound with concomitant generation of new signals due to byproducts. Table 1 shows further details for each peak with their respective identification, based on the National Institute of Standard (NIST) mass spectral library. In the TiO₂/UV degradation of propylene sulfide (Figure 2a) and trimethylene sulfide (Figure 2b), carbon dioxide was the only final product in the gas phase identified by MS (*m/z* 44). For thiophene (Figure 2c) and methyl disulfide (Figure 2d), the ions of *m/z* 64 and 48 are also present in the respective mass spectra. The identities of these ions were investigated using tandem mass spectrometry (MS/MS) and CID (24). The ion *m/z* 64 dissociates producing the fragments of *m/z* 48 and 32. Considering that *m/z* 64 corresponds to SO₂⁺, the fragment of *m/z* 48 (SO⁺) is generated by O loss and the fragment of *m/z* 32 (S⁺) by either O loss from SO⁺ (25) or O₂ loss from SO₂⁺. Because the fragment of *m/z* 48 also dissociates to *m/z* 32, it is not possible to determine whether the ion of *m/z* 48 results from dissociation of SO₂⁺ (*m/z* 64) or direct ionization of SO. However, thiophene photodegradation experiments monitored by chemical ionization mass spectrometry (Figure 3) proved that the ionic fragment of *m/z* 48 is formed directly from neutral SO. Before UV-irradiation, only protonated thiophene (*m/z* 85) is observed in the CI mass spectrum (Figure 3a). After partial photodegradation (Figure 3b), signals corresponding to protonated SO₂ (SO₂H⁺) of *m/z* 65 and protonated SO (SOH⁺) of *m/z* 49 are also detected. Note that no dissociation of SO₂H⁺ to SOH⁺ is expected due to the mild chemical ionization conditions and the highly unfavorable O loss from the closed-shell ion SO₂H⁺. For methyl disulfide however, EI-MS monitoring showed that only SO₂ is produced (spectra not shown).

Figure 4 shows the MS-SIM profile of the online monitoring of TiO₂/UV degradation of methyl disulfide (Figure 4a), thiophene (Figure 4b), propylene sulfide (Figure 4c), and trimethylene sulfide (Figure 4d). As the UV light is turned on, the concentration of the sulfur-containing compounds

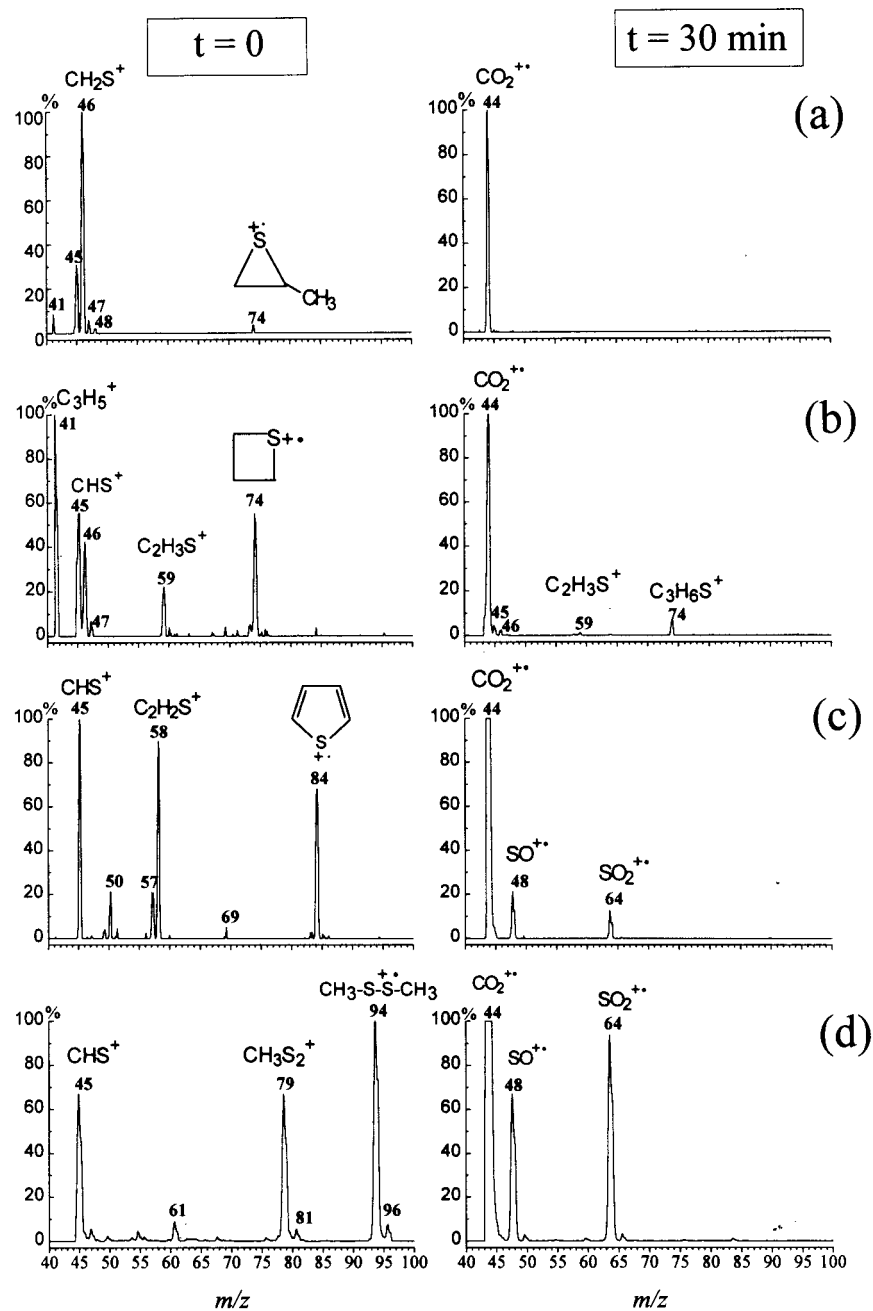


FIGURE 2. EI mass spectra (70 eV) of the gaseous synthetic air mixture containing (a) propylene sulfide, (b) trimethylene sulfide, (c) thiophene, and (d) methyl disulfide compounds before and after 30 min of UV-irradiation. Experimental conditions: 30 W black-light lamp, 21% oxygen, and 23% relative humidity.

decreases rapidly with the concomitant generation of carbon dioxide. The ions of m/z 48 and 64 have also been used to monitor the photodegradation of methyl disulfide (Figure 4a) and thiophene (Figure 4b). Note that in Figure 4a, SO^+ is produced mainly from dissociation of the SO_2^{++} ion, whereas in Figure 4b, SO^+ corresponds both to dissociation of SO_2^{++} and direct ionization of SO.

Table 2 summarizes the results obtained in the gas-phase photocatalytic destruction of all four sulfur-containing compounds under optimized conditions. High conversion yields (>99%) were obtained for propylene sulfide and trimethylene sulfide, with complete mineralization to CO_2 and SO_4^{2-} , as shown by carbon and sulfur mass balance. In the photodegradation of methyl disulfide and thiophene, SO_2 was detected as an additional byproduct. For methyl disulfide, 100% sulfur mass balance was achieved. For thiophene, however, sulfur mass balance reached 88% only,

and this low sulfur yield can be attributed to SO formation (not quantified), as demonstrated by the CI-MS analysis. For methyl disulfide and thiophene, CO_2 could not be quantified due to the interference of SO_2 in the Conductometry-Flow Injection-Analysis (FIA). Sulfur dioxide also diffuses through the PTFE, yielding conductance signals.

Although there are very few papers on the literature dealing with the destruction of sulfur-containing compounds using the photocatalytic process, recently, Peral and Ollis (26) using TiO_2/UV process obtained 10% conversion in the destruction of the dimethyl sulfide. The authors did not detect any sulfur compound on the TiO_2 , which was attributed to either the formation of SO_2 or SO_3 or to the formation of another mercaptan. Suzuki (12), using a honeycomb type of gaseous reactor, found that the destruction rates of S-compounds (CH_3SH and H_2S) were in the range of 0.13 min^{-1} .

TABLE 1. Major Ions in the 70 eV EI Mass Spectra of Sulfur Containing Compounds

Precursor	Name	m/z (relative abundance)
	trimethylene sulfide	41 (100), 45 (53), 46 (39), 47 (7), 59 (21), 74 (53)
	propylene sulfide	41 (8), 45 (35), 46 (100) 47 (5), 48 (3), 74 (3)
CH ₃ -S-S-CH ₃	methyl disulfide	45 (67), 61 (10), 79 (67), 81 (5), 94 (100), 96 (10)
	thiophene	45 (100), 50 (20), 57 (20), 58 (91), 69 (6), 84 (69)
SO ₂	sulfur dioxide	32 (11), 48 (50), 64 (100)
SO	sulfur oxide	32 (20) 48 (100)

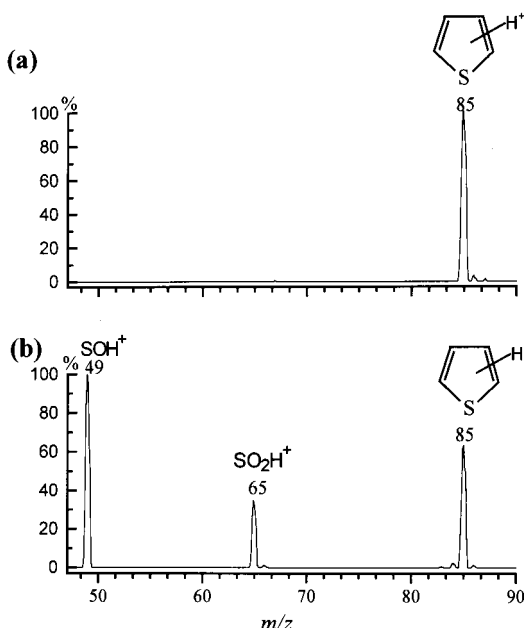
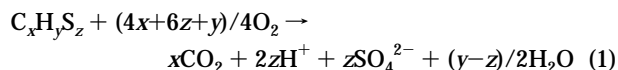


FIGURE 3. Methane-Cl mass spectra of TiO₂/UV degradation of thiophene (a) before and (b) during UV-irradiation.

The general equations for the complete photocatalytic conversion of sulfur-containing compounds may be described by the following stoichiometry



and could be applied to trimethylene sulfide and propylene, but for thiophene and methyl disulfide, the formation of SO₂ and SO as byproducts altered the reaction stoichiometry. For 1 mol of thiophene, 0.82 mol of sulfate ions, 0.06 mol of

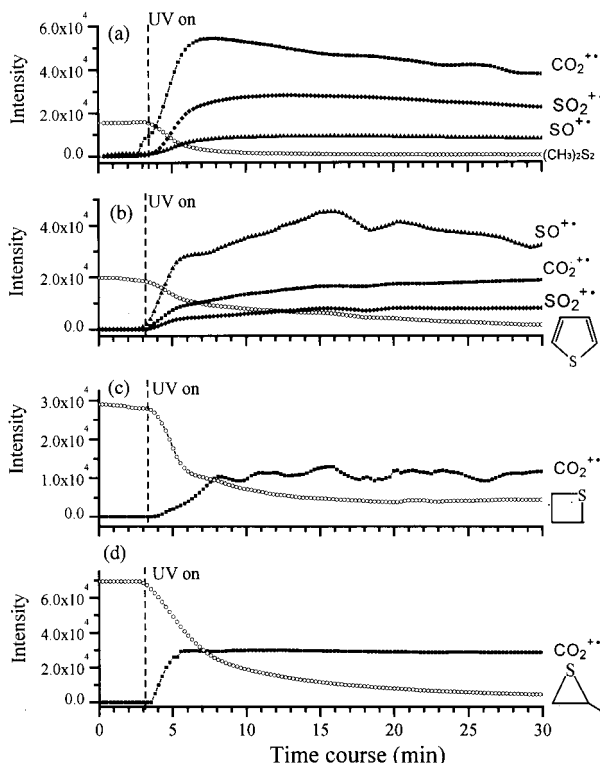
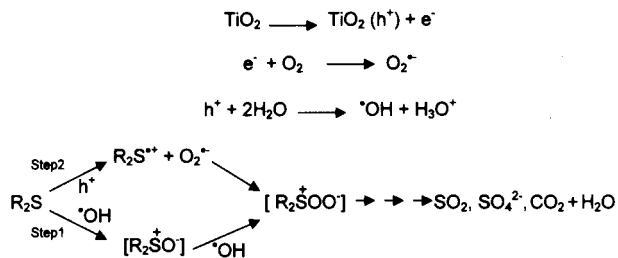


FIGURE 4. Diagrams of SIM-MS monitoring of TiO₂/UV degradation of methyl disulfide (a), thiophene (b), propylene sulfide (c), and trimethylene sulfide (d): (○) target compounds, (■) m/z 44 (CO₂⁺⁺), (▲) m/z 48 (SO⁺⁺), and (◆) m/z 64 (SO₂⁺⁺). Dashed lines indicate the time when the reactor was turned on.

SCHEME 1



sulfur dioxide, and 0.12 mol of sulfur oxide were generated. For 1 mol of methyl disulfide however, 1.53 mol of sulfate ions and 0.47 mol of sulfur dioxide were generated.

The formation of different radicals from the illumination of TiO₂ in water is well established in the literature (6). Both positive holes and hydroxyl radicals have been proposed as the oxidizing species responsible for initiating the attack on organic solutes. In Scheme 1 we show a proposed mechanism with the parallel reaction paths for both positive holes and hydroxyl radicals. When photocatalytic oxidation is conducted in the presence of water, the primary product of the electron transfer is often an adsorbed hydroxyl radical (step

TABLE 2. Initial Conditions and Sulfur-Containing Compounds Degradation Rates

substrate	C _{inlet} (ppmv)	res. time (min)	flow (mL/min)	conv (%)	oxid rate (μmol/min)	SO ₄ ²⁻ rate (μmol/min)	SO ₂ rate (μmol/min)	CO ₂ rate (μmol/min)	sulfur balance (%)	carbon balance (%)
trimethylene sulfide	61	1.81	262	99	0.72	0.71	nd	2.16	99	100
propylene sulfide	86	0.99	409	99	1.58	1.58	nd	4.65	100	98
thiophene	54	1.30	324	99	0.79	0.65	0.05	a	88	a
methyl disulfide	34	0.85	474	99	0.72	0.55	0.17	a	100	a

^a CO₂ analysis was not carried out due to SO₂ interference in the Conductometry-Flow Injection-Analysis (FIA).

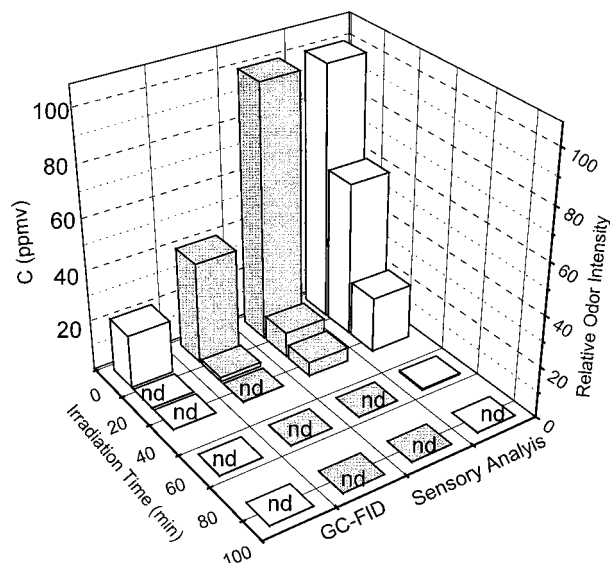


FIGURE 5. Performance of the TiO_2/UV process in the destruction of propylene sulfide (white) and trimethylene sulfide (black) as monitored by GC-FID and sensory analysis: nd = not detectable.

1). Long known for its high reactivity, this species can attack the sulfur-containing organic compounds generating the oxidation products as sulfoxides and sulfones. In another way (step 2), the photogenerated hole localized at the surface of the irradiated semiconductor is trapped by an adsorbed sulfur-containing organic compound, generating an adsorbed cation radical. The formation of a sulfur radical cation has been previously reported by Davidson and Pratt (27) and Fox and Abdel-Wahab (28, 29) in the presence of oxidatively inert solvents. In the experimental conditions used in this work it was not possible to detect either sulfoxides or sulfones (intermediates) because gas-phase reactions are very fast, generating as final products SO_2 and SO_4^{2-} as shown by the mass balance.

Although sulfate ions formed during the photocatalytic process were adsorbed onto the catalyst surface, no catalytic deactivation was observed in these experiments. Using H_2S , Canela et al. (13) showed that sulfate ions adsorbed onto TiO_2 promoted a decrease in the photocatalytic activity when high concentrations of H_2S (600 ppmv; corresponding to $5.4 \mu\text{mol min}^{-1}$ of SO_4^{2-}) were used. However, at 217 ppmv ($1.9 \mu\text{mol min}^{-1}$ of SO_4^{2-}) of H_2S , the photocatalytic activity was maintained for 24 h of continuous use. For all the sulfur-containing compounds tested in the present work, the maximum sulfate ions load observed was $1.58 \mu\text{mol min}^{-1}$, as shown in Table 2.

A comparative performance of the analytical technique used to monitor the target compounds (GC-FID) versus the sensory analysis is shown in Figure 5. Both GC-FID and sensory analysis indicate that the photocatalytic process was efficient to destroy the malodorous compounds. The panelists were unable to detect odor for both methylene sulfide and propylene sulfide in the outlet reactor, within 60 min after of the irradiation. On the other hand, using chromatographic analysis, after 15 min, it was not possible to detect the target compound in the outlet reactor. This result emphasizes the importance of sensory analysis in the evaluation process of destruction of malodorous compounds.

Acknowledgments

Financial support from the Fundação de Amparo à Pesquisa do Estado de São Paulo (FAPESP) (Grants 97/01545-6, 97/00758-6, 95/9497-5, and 97/6172-3) and the Conselho Nacional de Desenvolvimento Científico e Tecnológico (CNPq) are greatly acknowledged.

Literature Cited

- (1) Lutz, M.; Davidson, S.; Stowe, D. *Water Environ. Technol.* **1995**, *6*, 52–57.
- (2) Bonnin, C.; Laborie, A.; Paillard H. *Water Sci. Technol.* **1990**, *22*, 65–74.
- (3) Hwang, Y.; Matsuo, T.; Hanaki, K.; Suzuki, N. *Water Res.* **1995**, *29*, 711–718.
- (4) Young, W. F.; Horth, H.; Crane, R.; Ogden, T.; Arnott, M. *Water Res.* **1996**, *30*, 331–340.
- (5) Mills, B. *Filtration Separation* **1995**, *02*, 147–152.
- (6) Hoffman, M. R.; Martin, S. T.; Choi, W.; Bahnemann, D. W. *Chem. Rev.* **1995**, *95*, 69–96.
- (7) Mills, A.; Hunte, S. L. *J. Photochem. Photobiol., A* **1997**, *108*, 1–35.
- (8) Alberici, R. M.; Jardim, W. F. *Appl. Catal., B* **1997**, *14*, 55–68.
- (9) Dibble, L. A.; Raupp, G. B. *Environ. Sci. Technol.* **1992**, *26*, 492–495.
- (10) Peral, J.; Ollis, D. F. *J. Catal.* **1992**, *136*, 554–565.
- (11) Suzuki, K.; Satoh, S.; Yoshida, T. *Denki Kagaku* **1991**, *59*, 521–523.
- (12) Suzuki, K. In *Photocatalytic Air Purification on TiO_2 Coated Honeycomb Support*; Ollis, D. F., Al-Ekabi, H., Eds.; Elsevier: Amsterdam; 1993; Photocatalytic Purification and Treatment of Water and Air, Vol. 3, p 421.
- (13) Canela, M. C.; Alberici, R. M.; Jardim, W. F. *J. Photochem. Photobiol., A* **1998**, *112*, 73–80.
- (14) Lu, G.; Linsebigler, A. L.; Yates, J. T., Jr. *J. Phys. Chem.* **1995**, *99*, 7626–7631.
- (15) Lu, G.; Linsebigler, A. L.; Yates, J. T., Jr. *J. Chem. Phys.* **1995**, *102*, 4657–4662.
- (16) Raupp, G. B.; Junio, C. T. *Appl. Surf. Sci.* **1993**, *72*, 321–327.
- (17) Wong, J. C. S.; Linsebigler, A. L.; Lu, G.; Fan, J.; Yates, J. T., Jr. *J. Phys. Chem.* **1995**, *99*, 335–344.
- (18) Juliano, V. F.; Gozzo, F. C.; Eberlin, M. N.; Kascheres, C. *Anal. Chem.* **1996**, *68*, 1328–1334.
- (19) Eberlin M. N. *Mass Spectrom. Rev.* **1997**, *16*, 113–144.
- (20) *Standard Methods for the Examination of Water and Wastewater*, 18th ed.; Greenberg, A. S., Clesceri, I. S., Eaton, A. D., Eds.; American Public Health Association: Washington, DC, 2.19–2.23 (section 2170, Flavor Profile Analysis), 4.126–4.132 (4500- SO_4^{2-}), 1992.
- (21) West, P. W.; Gaeke, G. C. *Anal. Chem.* **1956**, *28*, 1816–1819.
- (22) Jardim, W. F.; Guimarães, J. R.; Allen, H. E. *Ciência Cultura* **1991**, *43*, 454–456.
- (23) Damásio, M. H.; Costell, E. *Rev. Agroquím. Tecnol. Aliment.* **1991**, *31*, 165–178.
- (24) Bush, K. L.; Glish, G. L.; McLuckey, S. A. *Mass Spectrometry/Mass Spectrometry Techniques and Applications of Tandem Mass Spectrometry*; VCH Publishers: 1989.
- (25) Sparrapan, R.; Mendes, M. A.; Ferreira, I. P. P.; Eberlin, M. N.; Santos, C.; Nogueira, J. C. *J. Phys. Chem. A* **1998**, *102*, 5189–5195.
- (26) Peral, J.; Ollis, D. F. *J. Mol. Catal. A* **1997**, *115*, 347–354.
- (27) Davidson, R. S.; Pratt, J. E. *Tetrahedron Lett.* **1983**, *24*, 5903–5906.
- (28) Fox, M. A.; Abdel-Wahab, A. A. *Tetrahedron Lett.* **1990**, *31*, 4533–4536.
- (29) Fox, M. A.; Abdel-Wahab, A. A. *J. Catal.* **1990**, *126*, 693–696.

Received for review April 20, 1998. Revised manuscript received April 30, 1999. Accepted May 20, 1999.

ES980404F